Metabolic and Transcriptomic Phenotyping of Inorganic Carbon Acclimation in the Cyanobacterium *Synechococcus elongatus* PCC 7942[1][W]

Doreen Schwarz, Anke Nodop, Jan Hüge, Stephanie Purfürst, Karl Forchhammer, Klaus-Peter Michel, Hermann Bauwe, Joachim Kopka, and Martin Hagemann*

Universität Rostock, Institut Biowissenschaften, Pflanzenphysiologie, D–18059 Rostock, Germany (D.S., S.P., H.B., M.H.); Lehrstuhl für Molekulare Zellphysiologie, Universität Bielefeld, D–33615 Bielefeld, Germany (A.N., K.-P.M.); Max-Planck-Institut für Molekulare Pflanzenphysiologie, 14476 Golm, Germany (J.H., J.K.); and Lehrstuhl für Mikrobiologie und Organismische Interaktion, Universität Tübingen, D–72076 Tuebingen, Germany (K.F.)

The amount of inorganic carbon is one of the main limiting environmental factors for photosynthetic organisms such as cyanobacteria. Using *Synechococcus elongatus* PCC 7942, we characterized metabolic and transcriptomic changes in cells that had been shifted from high to low CO_2 levels. Metabolic phenotyping indicated an activation of glycolysis, the oxidative pentose phosphate cycle, and glycolate metabolism at lowered CO_2 levels. The metabolic changes coincided with a general reprogramming of gene expression, which included not only increased transcription of inorganic carbon transporter genes but also genes for enzymes involved in glycolytic and photorespiratory metabolism. In contrast, the mRNA content for genes from nitrogen assimilatory pathways decreased. These observations indicated that cyanobacteria control the homeostasis of the carbon-nitrogen ratio. Therefore, results obtained from the wild type were compared with the MP2 mutant of *Synechococcus* 7942, which is defective for the carbon-nitrogen ratio-regulating PII protein. Metabolites and genes linked to nitrogen assimilation were differentially regulated, whereas the changes in metabolite concentrations and gene expression for processes related to central carbon metabolism were mostly similar in mutant and wild-type cells after shifts to low-CO_2 conditions. The PII signaling appears to down-regulate the nitrogen metabolism at lowered CO_2, whereas the specific shortage of inorganic carbon is recognized by different mechanisms.

Inorganic carbon (C_i) is converted into organic carbon (C) by photoautotrophic organisms utilizing light energy. Cyanobacteria represent a globally important group of such organisms. The cyanobacteria were the first oxygenic phototrophs that started to generate the oxygen-rich atmosphere on this planet. Moreover, their endosymbiotic engulfment by eukaryotic cells gave rise to algae and plants, the dominating photoautrophic organisms today (Knoll, 2008). However, cyanobacteria remain responsible for a high percentage of the annual primary production of organic biomass and represent a major sink for the greenhouse gas CO_2 in open oceans (Campbell et al., 1997).

In aquatic ecosystems, the amount of C_i is fluctuating and often not present in high enough quantities to satisfy the high demand of the main carboxylating enzyme, Rubisco. Therefore, cyanobacteria and many eukaryotic algae have evolved a carbon-concentrating mechanism (CCM) to increase the cellular C_i content. The cyanobacterial CCM employs several uptake systems for the C_i forms bicarbonate, which dominates in the alkaline oceans, and CO_2, leading to an accumulation of bicarbonate inside the cell. Bicarbonate enters a special compartment, the carboxysome, where Rubisco is closely associated with the enzyme carbonic anhydrase, which converts bicarbonate into CO_2. The action of carbonic anhydrase results in high C_i inside the carboxysome, causing the saturation of Rubisco (Badger et al., 2006; Cot et al., 2008; Kaplan et al., 2008).

The CCM is tightly regulated. A set of high-affinity transport systems is induced when cells are shifted from experimentally elevated high CO_2 (HC) to low ambient CO_2 (LC) conditions. The increase of CCM activity during LC acclimation is mainly controlled by transcriptional regulation but seems also to involve posttranscriptional regulation of enzyme activity. Signaling is rather poorly understood. At least three transcriptional factors, CmpR, NdhR, and AbrB-like proteins, were found to be involved in the up-regulation

[1] The work was supported by a grant from the Deutsche Forschungsgemeinschaft to M.H. and J.K.

* Corresponding author; e-mail martin.hagemann@uni-rostock.de.

The author responsible for distribution of materials integral to the findings presented in this article in accordance with the policy described in the Instructions for Authors (www.plantphysiol.org) is: Martin Hagemann (martin.hagemann@uni-rostock.de).

[W] The online version of this article contains Web-only data.

www.plantphysiol.org/cgi/doi/10.1104/pp.110.170225

of functionally defined gene groups (e.g. C_i transporters, NDH1 complexes, and photosynthetic complexes; Omata et al., 2001; Wang et al., 2004; Lieman-Hurwitz et al., 2009). Moreover, the affinity of the transcription factor CmpR for the *cmp* promoter was stimulated by the binding of 2-phosphoglycolate (2PG; Nishimura et al., 2008), the first metabolite of the photorespiratory 2PG metabolism (Eisenhut et al., 2008b). Possibly, 2PG (Marcus et al., 1983) and/or other photorespiratory intermediates could serve as metabolic signal(s) for C_i-limiting conditions (Kaplan et al., 2008).

Changes in C_i concentration affect N metabolism as well, because the cell depends on a balanced C-N ratio. The regulation of N acclimation is known in detail for some model strains of unicellular, nondiazotrophic cyanobacteria. In those cases, the transcriptional factor NtcA activates ammonia-repressed genes (Flores et al., 2005). The PII protein-based metabolic sensor system senses the cellular N levels and energy status by binding 2-oxoglutarate and ATP (Forchhammer, 2004, 2008). The two regulatory proteins, NtcA and PII, are functionally linked via the adaptor protein PipX, which mediates the signal transfer of the cellular C-N status to gene expression and adjusts the cellular metabolism to limiting N resources (Osanai and Tanaka, 2007; Llácer et al., 2010).

Initially, the CCM and its regulation as well as aspects of the N metabolism and its control were intensively studied using the model strain *Synechococcus elongatus* PCC 7942 (hereafter referred to as *Synechococcus* 7942; Kaplan and Reinhold, 1999). In recent years, another strain, *Synechocystis* sp. PCC 6803 (hereafter referred to as *Synechocystis* 6803), was the most commonly studied strain because its genome sequence had been published in 1996 (Kaneko et al., 1996). Based on this genome sequence, DNA microarrays were generated, allowing the characterization of global transcriptional changes, including studies of HC/LC shifts or acclimation to different light conditions (Hihara et al., 2001; Wang et al., 2004; Eisenhut et al., 2007). Later, the genome sequences and respective "omics" tools of *Synechococcus* 7942, as well as those of the almost identical strain PCC 6301, became accessible (for *Synechococcus* 7942, see http://www.ncbi.nlm.nih.gov/nuccore/NC_007604; for strain PCC 6301, see http://genome.kazusa.or.jp/cyanobase/PCC6301; Sugita et al., 2007; Nodop et al., 2008). Compared with *Synechocystis* 6803, the strain *Synechococcus* 7942 offers advantages for the analysis of C_i acclimation. *Synechococcus* 7942 is strictly photoautotrophic and cannot use organic C or N sources, whereas *Synechocystis* 6803 can also consume external Glc, making its overall metabolism more flexible but also more difficult to elucidate.

Here, we studied the HC/LC acclimation of *Synechococcus* 7942 using a combination of metabolomic and transcriptomic tools. Metabolic analyses of the primary metabolism using gas chromatography-mass spectrometry (GC-MS) were integrated with transcriptional phenotyping by whole-genome DNA microarrays. In addition to wild-type cells, we included the *Synechococcus* 7942 mutant MP2, which is defective in the PII protein-coding gene *glnB* (Forchhammer and Tandeau de Marsac, 1995). The data display a global picture of LC acclimation and signaling in *Synechococcus* 7942. Our results show that the PII protein is involved in LC acclimation but seems to be mainly responsible for the proper regulation of genes related to N assimilation.

RESULTS AND DISCUSSION

Physiological Characterization

To analyze the acclimation of *Synechococcus* 7942 to low C_i, HC-acclimated cells (grown for several days under 5% CO_2) of the wild type and the PII mutant MP2 were shifted to LC conditions (grown under 0.035% CO_2 by bubbling with ambient air), and samples were taken for metabolome and transcriptome characterization after 6 and 24 h. Growth conditions and sampling parameters were essentially the same as used before in our experiments with *Synechocystis* 6803 (Eisenhut et al., 2007, 2008a) to allow for comparison of the data sets. Under our culture conditions, wild-type cells grew better than the MP2 mutant (Fig. 1A). Approximately 33% lower growth rates were calculated for the mutant MP2 than wild-type cells. Growth retardation of MP2 under CO_2-enriched conditions was reported before (Forchhammer and Tandeau de Marsac, 1995). Moreover, the pigmentation of the MP2 mutant differed from that of wild-type cells. At HC conditions, mutant cells appeared more green-yellowish than did wild-type cells. This pigment change is mainly due to a reduced

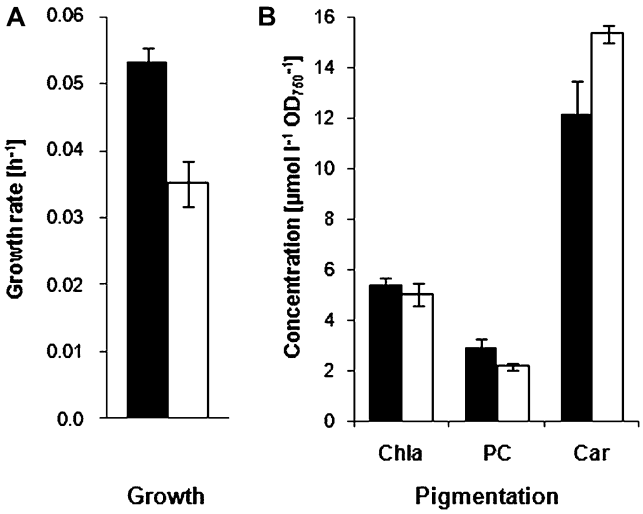

Figure 1. Growth and pigmentation of the *Synechococcus* 7942 wild type and the PII mutant. Growth rates (A) and pigmentation (B) of the *Synechococcus* 7942 wild type (black columns) and PII mutant (MP2; white columns) are shown for cells after long-term acclimation to HC (5% CO_2) conditions. Chla, Chlorophyll *a*; PC, phycocyanin; Car, carotenoids. Values shown are means and SD from four independent experiments.

content of phycobiliproteins and a slight increase in carotenoids in the cells of the MP2 mutant (Fig. 1B). Such a chlorotic phenotype is characteristic for cyanobacterial cells after N starvation (Sauer et al., 2001). It has been reported before that the PII mutant showed a reduced phycocyanin content and a lower protein-glycogen ratio compared with wild-type cells (Forchhammer and Tandeau de Marsac, 1995). Corresponding to a lower growth rate, the overall photosynthetic activity of HC-acclimated cells from the mutant MP2 was lower then that of wild-type cells (data not shown). However, we detected no significant differences in C_i affinity between cells of the *Synechococcus* 7942 wild type and the PII mutant. HC-acclimated cells are characterized by a half-saturating C_i concentration ($K_{1/2}$) for bicarbonate of approximately 150 μM (wild-type $K_{1/2}$ = 141.0 ± 31.6 μM, mutant MP2 $K_{1/2}$ = 166.8 ± 30.8 μM). The acclimation to LC increased the affinity toward bicarbonate approximately 4-fold in both cultures (wild-type $K_{1/2}$ = 35.5 ± 6.4 μM, mutant MP2 $K_{1/2}$ = 46.2 ± 19.6 μM). Previous studies revealed similar C_i affinities for HC cells (approximately 150 μM) that increased up to 10-fold during the first few hours after the shift from HC to LC conditions in *Synechococcus* 7942 (Woodger et al., 2003, 2005).

Changes in the Metabolome of Wild-Type Cells after Shifts from HC to LC Conditions

Using GC-MS, the metabolomes of wild-type and mutant MP2 cells were compared before and after shifts from HC to LC conditions. Among the several hundred metabolite signals detected, 85 metabolites could be identified and reproducibly quantified (Supplemental Table S1). This set of metabolites was evaluated to allow for a good survey of the central C and N metabolism of *Synechococcus* 7942. As expected, the shift to LC conditions resulted in an increased amount of 2PG, which reflects the stimulated oxygenase activity of Rubisco at the lowered CO_2-O_2 ratio (Fig. 2A). The other intermediates of the photorespiratory 2PG metabolism did not differ significantly when cells were acclimated to either LC or HC.

Marked changes were also observed to metabolites of the Calvin-Benson cycle, the associated glycolytic pathway, and the oxidative pentose-phosphate cycle (OPP). The primary C fixation product of Rubisco, 3-phosphoglycerate (3PGA), increased approximately 2.5-fold in LC-treated cells (Fig. 2B). A clear increase was also observed for 2-phosphoglycerate (2PGA) and phospho*enol*pyruvate (PEP). These two intermediates are likely synthesized from 3PGA via glycolytic reactions (Fig. 3), which might indicate an increased diversion of newly fixed organic C toward glycolysis. An increased flux of C from the Calvin-Benson cycle into the glycolytic pathway was recently shown with HC/LC-shifted cells of *Synechocystis* 6803 using ^{13}C-labeling experiments (Huege et al., 2011). For LC-shifted cells of *Synechococcus* 7942, this possibility is supported by the finding that the transcript levels of many

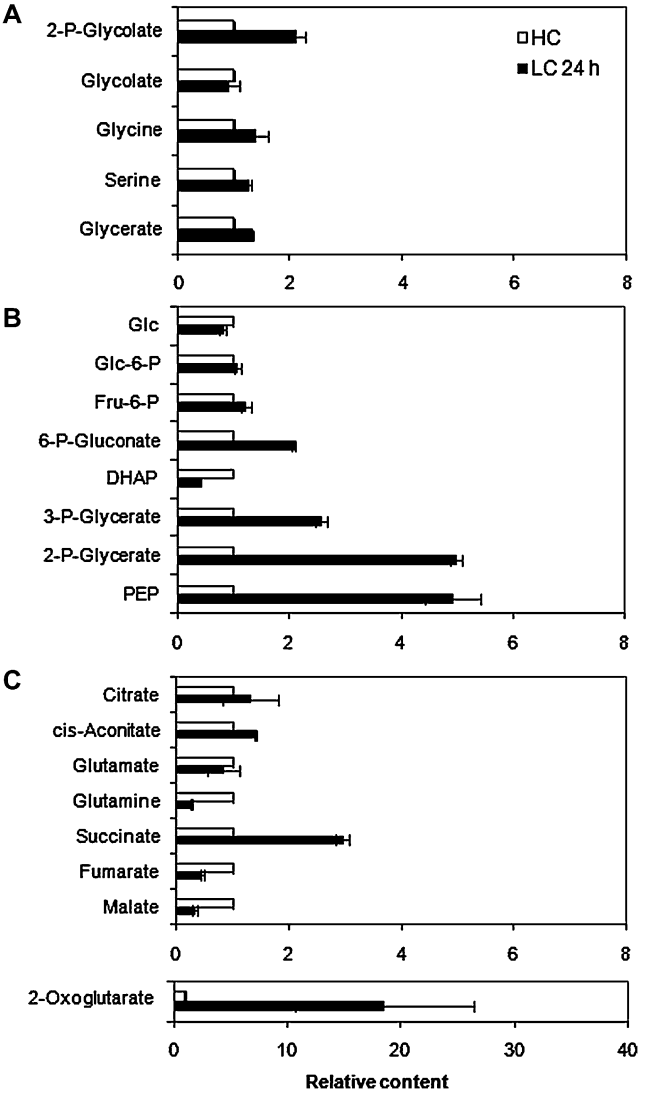

Figure 2. Changed metabolite levels in cells of the *Synechococcus* 7942 wild type (WT) in response to the shift from HC (5% CO_2) to LC (0.035% CO_2) for 24 h. A, Photorespiratory 2PG metabolism. B, Calvin-Benson cycle, OPP, and glycolysis. C, Incomplete TCA cycle and GS/GOGAT. Data shown are mean values of relative changes (HC value was set to 1) and SD of three biological and two technical replicates. DHAP, Dihydroxy acetonephosphate.

genes for glycolytic enzymes (see below) increased in parallel to the higher steady-state values of glycolytic intermediates. Moreover, the increased amount of 6-phosphogluconate in LC-shifted cells also indicates an increase of the OPP cycle, whereas other sugar phosphates, such as Glc-6-P and Fru-6-P (Fig. 2B), as well as Suc (Supplemental Table S1), remained almost unchanged. In contrast, in an experimental setup similar to the one chosen in our investigations, metabolite concentrations of the Calvin-Benson cycle did not change significantly in the plant Arabidopsis (*Arabidopsis thaliana*), with only the flux toward storage carbohydrates reduced under lowered CO_2 conditions (Arrivault et al., 2009).

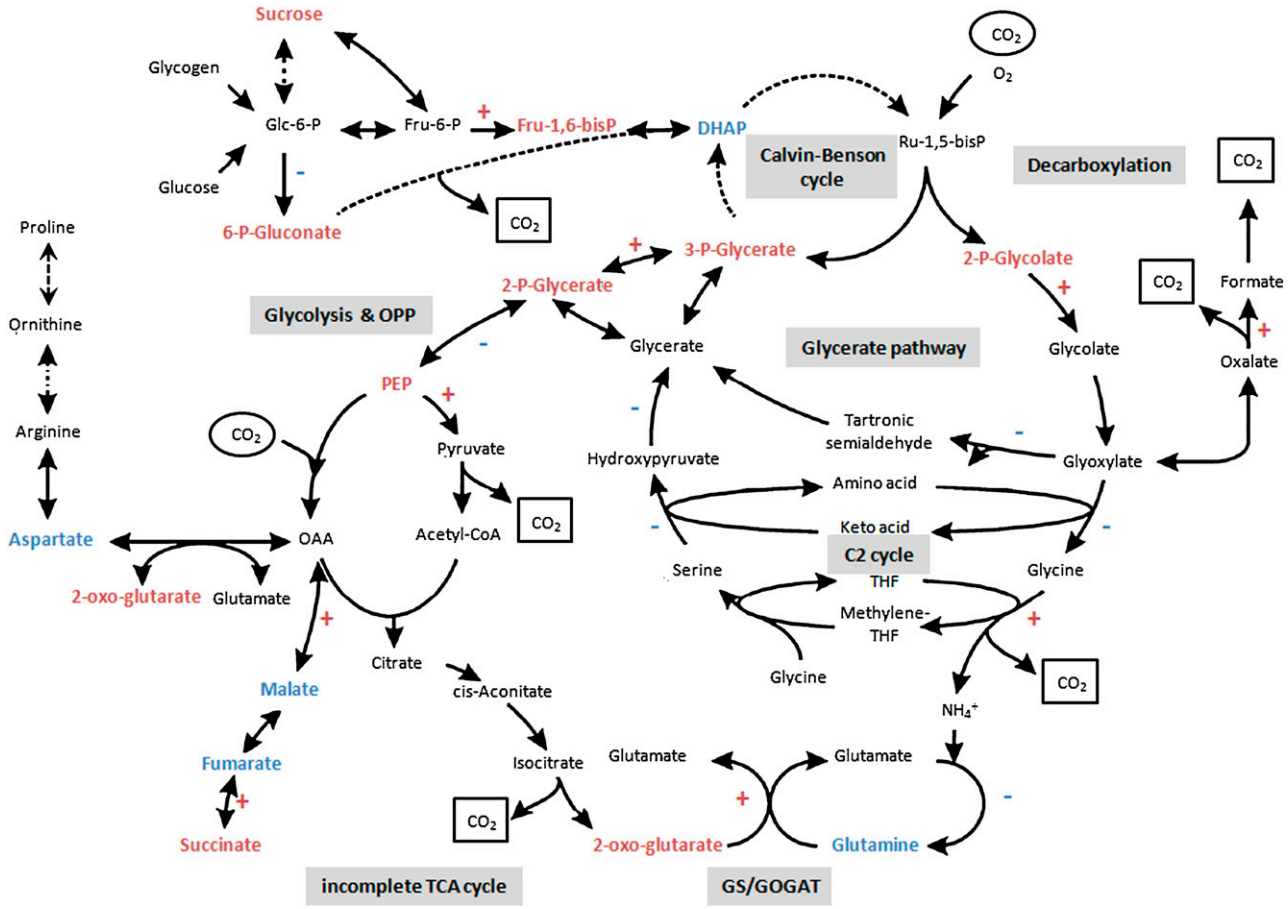

Figure 3. Central C and N metabolism in *Synechococcus* 7942. Significant alterations in the metabolic and transcriptomic pattern of wild-type cells after transfer from high CO_2 (5%) to low CO_2 (0.035%) are indicated. An increase in the pool size of a metabolite after shift to LC conditions is indicated by showing the compound in red, whereas a decreased metabolite is displayed in blue. Changes in the expression of genes of the corresponding enzymatic steps are indicated with symbols (+, increased transcription; −, decreased transcription) at the corresponding arrows.

Clear changes occurred in the levels of selected intermediates of the tricarboxylic acid (TCA) cycle. It is widely believed that the cyanobacterial TCA cycle is incomplete (Fig. 3) because of the missing 2-oxoglutarate (2OG) dehydrogenase complex and serves mainly to produce C skeletons for the linked amino acid biosynthesis (Luque and Forchhammer, 2008). Malate and fumarate pools dropped to 50% or less after the shift from HC to LC (Fig. 2C). Interestingly, the pool size of the end product of this branch of the incomplete TCA cycle, succinate, showed a clear increase after a shift to LC for 24 h. Similarly, but to a higher extent, the end product of the other branch of the incomplete TCA cycle, 2OG, also accumulated under LC conditions, whereas the precursors citrate and aconitate did not show significant changes. 2OG is probably mostly used as a C skeleton for subsequent N assimilation via the glutamine synthetase/glutamate synthase (GS/GOGAT) cycle (Fig. 3), leading to Glu, which is subsequently used as an amino donator or building block for other biosyntheses such as amino acids, chlorophylls, or heme/bilin. The amount of Gln, the primary N assimilation product in *Synechococcus* 7942, was reduced 3-fold at 24 h after the shift from HC to LC, but the level of Glu did not change (Figs. 2C and 4). The amount of Asp decreased significantly (Fig. 4). Since Asp is made from oxaloacetate, the decreased use of oxaloactetae for Asp synthesis is in agreement with its increased diversion into the succinate pool. Another possible explanation for the coordinated increase of 2OG and succinate is to assume the existence of a modified rather than open TCA cycle. Experimental work on *Synechocystis* 6803 (Cooley et al., 2000) and a metabolic network model for this cyanobacterial strain (Knoop et al., 2010) suggest that a shunt exists that closes the TCA cycle, which starts from 2OG, goes over Glu, 4-aminobutanoate, succinate-semialdehyde, and goes back to succinate. Regardless of whether the TCA cycle is open or somehow closed, the newly fixed organic C is accumulated throughout the path from 3PGA via 2PGA to PEP and subsequently into intermediates of the TCA cycle. A possible interpretation, which is also supported by transcriptomic evidence (see below), could be a

Table I. *Relative transcriptional changes of genes for enzymes involved in the primary C and N metabolism in cells of the Synechococcus 7942 wild type and the PII mutant (MP2) in response to shifts from HC to LC conditions for 6 or 24 h*

The relative expression (fold change) of these genes in the wild type and the MP2 mutant is given for cells grown at HC conditions (MP2-HC/WT-HC). Genes for enzymes of the phosphoglycolate metabolism, glycolysis, OPP cycle, incomplete TCA cycle, and N assimilation via GS/GOGAT were selected according to the annotation in CyanoBase or identified by protein BLAST searches with functionally characterized proteins from *Synechocystis* 6803. Significantly increased or decreased transcript levels (change of ≥1.87-fold and ≤0.53-fold) are shown in boldface.

Open Reading Frame	Gene Name	Annotation	WT-LC/WT-HC		MP2-HC/WT-HC	MP2-LC/MP2-HC	
			6 h	24 h		6 h	24 h
C2 cycle							
2613	*cbbZ*	Phosphoglycolate phosphatase	1.04	**2.00**	0.82	0.80	1.24
0217		Putative phosphoglycolate phosphatase	**6.22**	0.73	**2.15**	**3.27**	**0.26**
0276	*glcD1*	GlcD subunit	1.10	0.54	0.81	0.96	**0.12**
1718	*glcD2*	GlcD subunit	0.63	0.59	1.35	0.90	**2.36**
1717		GlcD subunit (Fe-S)	0.80	1.03	0.86	0.64	1.47
0191		Ser-glyoxylate transaminase	**0.41**	**0.42**	0.76	0.94	**0.14**
0282	*glyA*	Ser hydroxymethyltransferase	**0.51**	0.87	**0.47**	0.75	0.62
1501		D-3-Phosphoglycerate dehydrogenase	0.60	**0.40**	0.54	0.91	**0.30**
1347	*ddh*	2-Hydroxyacid dehydrogenase-like	0.79	**0.16**	0.99	0.99	**0.08**
Gly cleavage system							
2308	*gcvT*	Aminomethyltransferase, T-protein	1.05	**3.29**	**1.97**	1.18	**2.35**
2047	*gcvP*	Gly decarboxylase, P-protein	1.26	**0.41**	0.72	0.80	0.63
2046	*gcvH*	Gly dehydrogenase, H-protein	1.01	**2.15**	1.00	1.02	0.91
1198	*phdD*	Dihydrolipoamide dehydrogenase, L-protein	1.52	0.97	1.15	**1.89**	0.90
Glycerate pathway							
0139		Acetolactate synthase 3 catalytic subunit	0.74	**0.53**	1.12	1.16	**0.16**
1857		3-Hydroxyacid dehydrogenase	0.84	0.82	0.61	0.66	0.55
Complete decarboxylation							
2388		Oxalate decarboxylase	0.95	**2.24**	0.92	1.02	**3.41**
2387		Hypothetical protein (possible formate dehydrogenase)	1.00	1.37	1.85	1.14	**2.98**
Calvin-Benson cycle							
1742	*gap*	Glyceraldehyde-phosphate dehydrogenase	**0.30**	**0.07**	**0.42**	1.16	0.66
1939	*gap*	Glyceraldehyde-phosphate dehydrogenase	1.11	**3.05**	**2.34**	1.71	**2.22**
0245	*gap*	Glyceraldehyde-phosphate dehydrogenase	0.75	0.94	**0.49**	0.88	1.40
1116	*pgk*	Phosphoglycerate kinase	**0.45**	**0.35**	0.62	1.29	0.61
1261	*tpi*	Triosephosphate isomerase	1.14	**0.13**	1.19	0.92	**0.41**
Glycolysis and OPP							
2334	*zwf*	Glc-6-P dehydrogenase	1.26	**0.32**	**2.13**	1.05	**0.34**
2029	*pgi*	Glc-6-P isomerase	1.00	0.66	0.82	1.26	1.86
0592		6-Phosphofructokinase	0.81	**2.71**	**2.24**	0.81	**4.22**
0469		Phosphoglyceromutase	0.96	0.71	0.89	1.18	**0.28**
0485		Phosphoglycerate mutase	**0.46**	**2.74**	**0.43**	0.87	0.80
2078		Phosphoglycerate mutase	0.58	**15.42**	**8.78**	1.08	**1.90**
0639	*eno*	Phosphopyruvate hydratase	**0.43**	**0.43**	0.73	0.69	**0.14**
0098		Pyruvate kinase	0.86	**3.82**	1.61	1.19	0.91
0143		Pyruvate/2-oxoglutarate dehydrogenase (E1 component)	0.82	0.61	**0.41**	1.11	**0.36**
1944		Pyruvate dehydrogenase (lipoamide)	0.82	0.54	1.09	0.94	0.55
1068		Branched-chain α-keto acid dehydrogenase (E2 component)	0.94	**0.14**	1.28	0.97	**0.07**
2384	*nifJ*	Pyruvate:ferredoxin (flavodoxin) oxidoreductase	0.94	**3.54**	**2.72**	1.03	**2.01**
2252	*ppc*	PEP carboxylase	1.30	0.61	1.90	1.59	**1.96**
2545		Asp aminotransferase	0.88	1.20	0.59	1.02	1.06
1297		Malic enzyme	0.86	**2.86**	**0.46**	1.06	0.74
TCA cycle (incomplete)							
0612	*gltA*	Citrate synthase	0.73	1.72	**0.38**	1.21	**2.03**
0903	*acnB*	Aconitate hydratase	0.69	1.44	0.81	0.72	0.64
1719	*icd*	Isocitrate dehydrogenase	0.65	0.72	0.59	1.04	**0.23**
1007	*fumC*	Fumarate hydratase	**0.44**	0.97	**0.35**	0.77	1.40
0314		Succinate dehydrogenase, subunit C	0.96	0.83	0.93	0.75	**0.51**
0641	*sdhA*	Succinate dehydrogenase flavoprotein	1.24	**4.45**	**2.27**	1.57	1.35
1533	*sdhB*	Succinate dehydrogenase/fumarate reductase iron-sulfur subunit	**0.39**	1.11	1.11	0.69	1.51

(*Table continues on following page.*)

Table I. (*Continued from previous page.*)

Open Reading Frame	Gene Name	Annotation	WT-LC/WT-HC		MP2-HC/ WT-HC	MP2-LC/MP2-HC	
			6 h	24 h		6 h	24 h
GS/GOGAT							
0169		Glu-ammonia ligase, Gln synthetase type III	**0.53**	0.73	0.88	0.75	1.26
2156		L-Gln synthetase	**0.33**	**0.28**	**0.28**	0.88	0.74
2296		L-Gln synthetase	0.91	**0.21**	1.01	0.74	**0.19**
0890		Glu synthase (ferredoxin)	1.15	**1.90**	1.64	1.19	1.85

transiently inhibited or delayed N assimilation compared with C utilization through glycolysis and TCA reactions upon a shift from HC to LC. LC-treated cells may enhance the efficiency of C assimilation more rapidly than the efficiency of N assimilation or reutilization of inorganic N set free by LC-triggered photorespiration. Similar observations were made in Arabidopsis. In the leaves of this plant, the high energy-demanding N assimilation was also reduced under limiting CO_2 conditions (Arrivault et al., 2009).

Generally, the changes in metabolite profiles observed in HC/LC-shifted cells of *Synechococcus* 7942 resembled the previously reported metabolic changes in *Synechocystis* 6803 (Eisenhut et al., 2008a). In both strains, LC-shifted cells are characterized by higher levels of 2PG that accumulated also in LC-treated *Anabaena* cells (Marcus et al., 1983). We also found higher relative amounts of 6-phosphogluconate, 3PGA, 2PGA, PEP, and a remarkable increase in 2OG. 2OG was previously believed to be low in LC-shifted cells because these growth conditions increase the N-C ratio. This ratio was considered to be sensed by the PII protein via sensing the ATP and the 2OG pool sizes (Forchhammer, 2004). Under our culture conditions, 24 h after the shift to LC, the C_i fixation is decreased but the energy-consuming N assimilation is decreased even more drastically. These metabolic alterations are also clearly reflected in the transcriptional changes of the corresponding biosynthetic genes (see below). In contrast, a switch from high to low N, which should induce a shift from low to high C-N ratio conditions, is accompanied by an immediate decrease in the 2OG level and activation of the N assimilatory processes. These observations gave rise to the hypothesis that high 2OG levels are used as an indicator for N limitation (Muro-Pastor et al., 2001, 2005). In conclusion, the unexpected increase of the 2OG pool after shifts from high to low CO_2, which is accompanied by a relative increase in the N-C ratio, found here in *Synechococcus* 7942 and previously in *Synechocystis* 6803 (Eisenhut et al., 2008a), is in contrast to previous reports of the major role of 2OG as an indicator for N limitation (Muro-Pastor et al., 2005; Forchhammer, 2008). Whereas the metabolites of the 2OG branch of the incomplete TCA cycle responded consistently in *Synechococcus* 7942 and *Synechocystis* 6803, major differences were observed in the C4 branch of the TCA cycle: namely, succinate increased whereas malate and fumarate decreased in *Synechococcus* 7942 when shifted from HC to LC (Fig. 2), whereas malate and fumarate increased and succinate decreased in cells of *Synechocystis* 6803 (Eisenhut et al., 2008a) under similar experimental conditions.

Correlation of Metabolic with Transcriptomic Changes in Wild-Type Cells

The changes at the metabolite level reflect the complex changes of enzyme activities constituting primary metabolism. The transcriptomic part of the underlying regulatory mechanisms can be globally monitored. Fortunately, in bacteria, the majority of such regulatory changes are established via transcriptional control; however, as a note of caution, there are also indications that posttranscriptional regulation occurs (Völker and Hecker, 2005). Corresponding to the increased demand for photorespiratory 2PG detoxification, an increased transcript level of genes for putative 2PG phosphatases (*orf0217* and *orf2613*) was detected. The majority of the other genes coding for enzymes in the plant-like photorespiratory 2PG cycle (Kern et al., 2011) remained unchanged. Only transcripts for two subunits of the Gly cleavage system were found to be increased, and those for the Ser hydroxymethyltransferase gene were decreased (Table I). As shown before in *Synechocystis* 6803 (Eisenhut et al., 2008b), the *Synechococcus* 7942 genome also codes for enzymes that may constitute the plant-like (Kern et al., 2011) and alternative routes of 2PG metabolism (Table I). In addition to the increased expression of the starting enzyme, 2PG phosphatase, the genes constituting the alternative route of complete decarboxylation of glyoxylate showed higher transcript levels in *Synechococcus* 7942 wild-type cells after transfer to LC conditions, whereas the expression of genes of the bacterial-like glycerate pathway remained unchanged (Table I; Fig. 3). These responses were found previously in *Synechocystis* 6803 under identical conditions (Eisenhut et al., 2007). Based on this data set, the initial dephosphorylation of 2PG seems to be a crucial, possibly rate-liming step after a shift to LC, whereas the subsequent glycolate metabolism with the three branches appears to be mostly constitutively expressed and coordinated toward efficient detoxification and avoidance of significant accumulation of photorespiratory intermediates. The only exception is the complete decarboxylation route, which seems to represent an optional, LC-induced detoxification module in both *Synechococcus* 7942 and *Synechocystis* 6803.

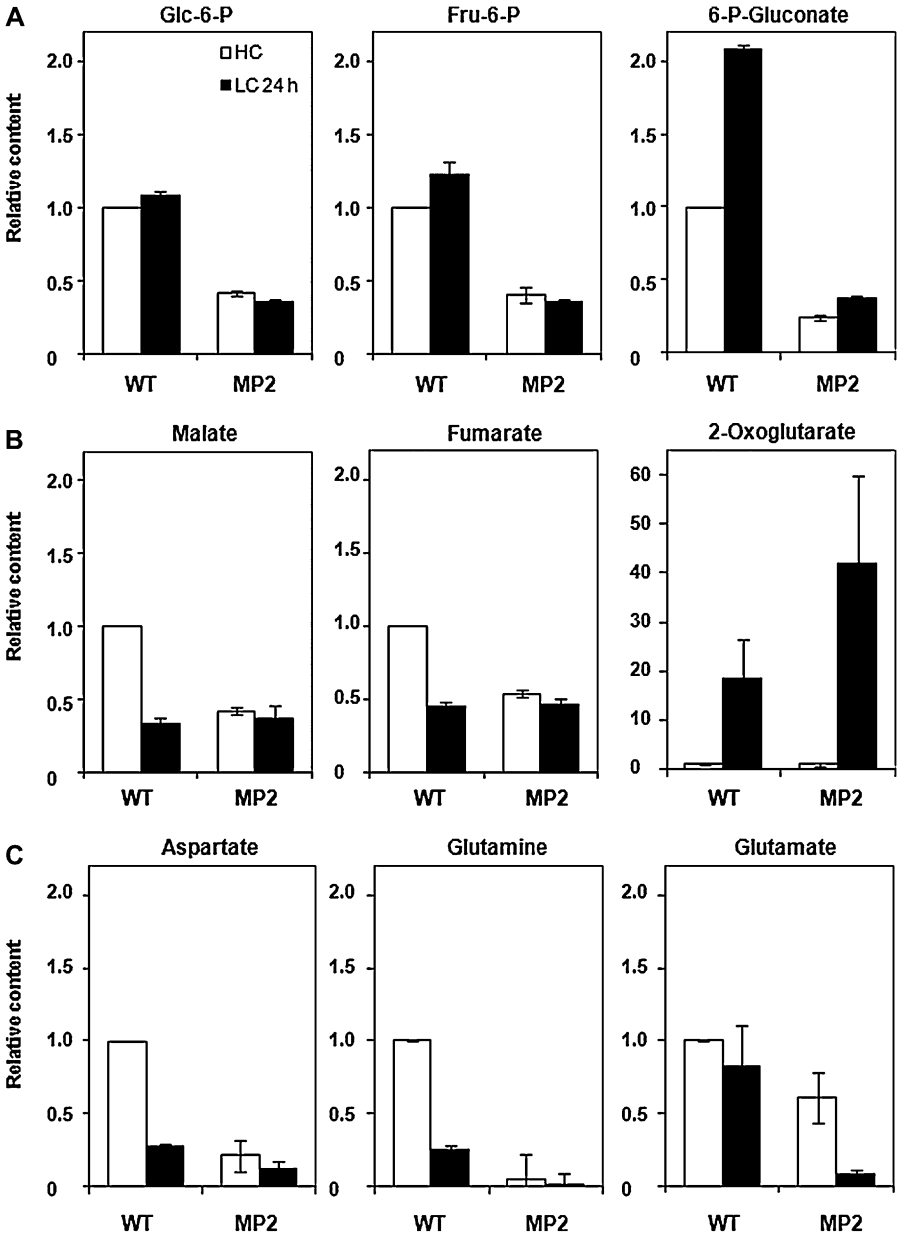

Figure 4. Metabolic changes in cells of *Synechococcus* 7942 wild type (WT) compared with the PII mutant (MP2) after shifts from HC (5% CO_2) to LC (0.035% CO_2) for 24 h. A, Glycolysis and OPP. B, Incomplete TCA cycle. C, GS/GOGAT. Data shown are mean values and SD of three biological and two technical replicates.

A shift to LC conditions probably decreases the Calvin-Benson cycle activity in *Synechococcus* 7942, which is reflected in decreased CO_2 assimilation (Mayo et al., 1989) and coincident accumulation of 3PGA. In addition to limited CO_2 availability for the Calvin-Benson cycle, 3PGA accumulation can also be explained by the observed 2PG accumulation, which is known to directly inhibit Calvin-Benson cycle enzymes, such as phosphofructokinase (Kelly and Latzko, 1977) and triosephosphate isomerase (Husic et al., 1987; Norman and Colman, 1991). Moreover, the expression of genes for enzymes of the reductive phase of the Calvin-Benson cycle, phosphoglycerate kinase, and one of the glyceraldehyde 3-phosphate dehydrogenase isoforms (*orf1742*), as well as for trisosephosphate isomerase, showed decreased mRNA levels in wild-type cells after the LC shift (Table I). This concerted response reflects the acclimation process toward diminished growth under reduced CO_2 availability. The accumulated 3PGA is obviously diverted into glycolysis and the OPP cycle rather than being used for storage as glycogen under HC. In parallel to 3PGA, the increases in 2PGA and PEP levels after the shift from HC to LC is correlated to the increased transcript level of related genes: namely *orf0485* and *orf2078*, which encode phosphoglycerate mutases for the conversion of 3PGA into 2PGA. Furthermore, the transcript levels of the pyruvate kinase-encoding gene *orf0098* and the gene *orf2384*, which encodes a component of the pyruvate dehydrogenase, are also approximately 3.5-fold increased after the long-term LC shift. However, the gene for PEP carboxylase (*ppc*; *orf2252*) did not

change expression under LC conditions (Table I), as reported previously (Woodger et al., 2003). It may further be hypothesized that the glyceraldehyde-3-phosphate dehydrogenase isoform encoded by *orf1939* is implicated in the glycolytic pathway rather than in the Calvin-Benson cycle. The expression changes observed for this gene are correlated to the detected changes in metabolite contents or mRNA levels of other genes specific to the glycolytic pathway, which are accumulated in wild-type cells shifted to LC (Table I).

The redirection of organic C from glycogen storage under HC conditions to increased utilization by N assimilation and/or respiration is also reflected by the increased amounts of TCA cycle intermediates. The glycolysis and TCA cycle are connected via the conversion of pyruvate to acetyl-CoA, a reaction that generates CO_2. CO_2 is also released in the TCA cycle step that converts isocitrate into 2OG (Fig. 3). Interestingly, the amount of mRNA of the gene for malic enzyme, which may regenerate pyruvate from excess malate in the incomplete TCA cycle, is also increased in wild-type cells 24 h after the LC shift. The probable increased activity of malic enzyme could also explain the rather low level of malate compared with succinate and the higher amount of pyruvate under LC conditions.

Corresponding to the increased levels of TCA cycle intermediates, the genes for some enzymes of this cycle also showed an increased mRNA level (Table I), such as *orf0612* (citrate synthase) and *orf0641* (succinate dehydrogenase flavoprotein subunit), but these changes appear to be insufficient to explain the accumulation of succinate and 2OG reported above. However, genes coding Gln synthetase, the essential enzyme involved in consuming 2OG in the GS/GOGAT cycle, are also repressed when cells are shifted to LC (Table I). In addition to the lowered transcript level, the Gln synthetase activity also seems to be decreased, as the mRNA levels of genes for the Gln synthetase inhibitory proteins (García-Domínguez et al., 1999), GifA (*orf0900*) and GifB (*orf2529*), are also clearly enhanced 6 h after the transfer from HC into LC conditions (Table II). Obviously, the coordinated regulation of gene expression and enzyme activities are in agreement with the concurrently decreased Gln and increased 2OG levels (Fig. 2).

Interestingly, although all other enzymes of the incomplete TCA cycle known from cyanobacteria are annotated (CyanoBase; http://genome.kazusa.or.jp/cyanobase/SYNPCC7942), the genome of *Synechococcus* 7942 apparently lacks a gene for a specific malate dehydrogenase. This feature could explain the different responses of *Synechococcus* 7942 compared with *Synechocystis* 6803 in this branch of the TCA cycle after shifts from HC to LC conditions. However, it can be assumed that another, unspecific dehydrogenase could be able to convert malate into oxaloacetate.

In contrast to the closely linked changes of the metabolite and transcript levels involved in the glycolysis and TCA cycle, the increase in 6-phosphogluconate is not accompanied by an increased/decreased expression of enzymes of the OPP cycle in cells shifted for 6 h to LC conditions.

Comparison of the Metabolome of the Wild Type and PII Mutant after Shifts from HC to LC Conditions

Cells of the wild type and the PII mutant of *Synechococcus* 7942 were investigated under identical conditions in order to study the effect of a defective C-N sensor on LC acclimation. Generally, the metabolic patterns and most LC-induced changes were similar in wild-type and mutant cells with respect to the intermediates of the photorespiratory 2PG metabolism, Calvin-Benson cycle, and the glycolytic pathway (Supplemental Table S1). However, differences were observed when mutant cells were grown at HC conditions. The MP2 mutant seems to divert a higher amount of C into the Suc pool (Supplemental Table S1). This process appears to occur at the expense of the respective precursor pools, Glc-6-P and Fru-6-P, as well as 6-phosphogluconate from the sugar-catabolizing OPP pathway (Fig. 4A). These findings correspond to the reported increase in the glycogen-protein ratio of this mutant (Forchhammer and Tandeau de Marsac, 1995). Moreover, the amounts of the TCA cycle intermediates malate and fumarate and the major amino acids Glu, Gln, and Asp are clearly reduced in cells of the MP2 mutant under HC conditions (Fig. 4, B and C). These changes indicate a reduced capability for N assimilation in the PII mutant, explaining the slight bleaching phenotype of the mutant cells (Fig. 1B). Interestingly, the reduced levels of the mentioned TCA cycle intermediates and amino acids in the mutant MP2 at HC are almost identical to the lowered levels of these intermediates observed in wild-type cells when shifted to LC for 24 h (Fig. 4). Obviously, the mutant MP2 is unable to correctly sense the prevailing C-N ratio (i.e. at the level of TCA cycle metabolites and those connected to it, the PII mutant seems to be locked into an N-limiting state, which also begins to appear during the first few hours after LC shifts in wild-type cells). While the TCA cycle intermediates are not further diminished in the LC-shifted cells of mutant MP2 compared with HC, the amounts of Glu, Asp, and Gln became further reduced under LC conditions. The decreased amino acid levels correspond to the increase in the 2OG precursor pool in LC-shifted cells of the mutant MP2, which clearly exceeds the increase observed before in LC-shifted wild-type cells (Fig. 4B). Possibly, the regulatory role of the PII protein extends toward regulation of the incomplete TCA cycle for 2OG production, appropriate for the demands of the connected N assimilation and respective amino acid biosyntheses. In contrast, the central C metabolism (i.e. Calvin-Benson cycle, glycolysis, OPP cycle, and glycogen biosynthesis) should be controlled by other, noncharacterized regulators at different C_i levels. The metabolites of these pathways changed similarly in LC-shifted wild-type cells as well as PII

Table II. *Relative transcriptional changes of genes for proteins involved in the CCM and other highly regulated genes in cells of the Synechococcus 7942 wild type and the PII mutant (MP2) shifted from HC to LC conditions for 6 or 24 h*

The relative expression of these genes in the wild type and the MP2 mutant is given for cells grown at HC conditions (WT-HC/MP2-HC). Genes for proteins of the bicarbonate transporters BCT1 and SbtA, alternative NDH1 complexes, the shell of the carboxysome, Rubisco, and carbonic anhydrase were selected according to the annotation in CyanoBase or identified by protein BLAST searches with functionally characterized proteins from *Synechocystis* 6803. Significantly increased or decreased transcript levels are shown in boldface.

Open Reading Frame	Gene Name	Annotation	WT-LC/WT-HC		MP2-HC/ WT-HC	MP2-LC/MP2-HC	
			6 h	24 h		6 h	24 h
BCT1							
1488	*cmpA*	Bicarbonate transport membrane protein	**24.69**	0.86	1.44	**33.71**	1.18
1489	*cmpB*	Bicarbonate transport permease	**21.44**	0.79	1.40	**28.41**	1.55
1490	*cmpC*	Bicarbonate transport ATP-binding subunit C	**13.36**	**0.49**	1.01	**17.03**	1.10
1491	*cmpD*	Bicarbonate transport ATP-binding subunit D	**17.83**	0.88	1.52	**19.34**	**1.96**
1310	*cmpR*	Transcriptional regulator for *cmp/ndh3* operons	**2.47**	1.11	0.66	**7.14**	0.86
SbtA							
1475	*sbtA*	Sodium-dependent bicarbonate transporter	**15.45**	0.57	0.98	**27.11**	—
1476		Hypothetical protein	**3.85**	**0.20**	0.73	**3.92**	**0.41**
NDH1							
2091	*ndhF3*	NAD(P)H-quinone oxidoreductase subunit F	1.27	**0.03**	**2.23**	1.34	**0.14**
2092	*ndhD3*	NAD(P)H-quinone oxidoreductase subunit D, chain M	**9.87**	1.37	1.43	**15.09**	**2.55**
2093	*cupA*	CO_2 hydration protein	**8.66**	1.20	**2.15**	**15.38**	**2.71**
2094		β-Ig-H3/fasciclin	**10.88**	**2.11**	**2.49**	**14.02**	—
0309	*ndhF4*	NAD(P)H-quinone oxidoreductase subunit F	1.09	**0.10**	1.47	0.62	**0.10**
0609	*ndhD4*	NAD(P)H-quinone oxidoreductase subunit D, chain M	0.88	1.00	0.62	1.50	1.60
0308	*cupB*	CO_2 hydration protein	1.50	1.01	**0.50**	1.12	1.70
Shell proteins							
1421	*ccmK1*	Putative carboxysome assembly protein	1.72	**0.03**	0.96	**2.72**	0.86
1422	*ccmL*	CO_2-concentrating mechanism protein CcmL	1.70	**0.16**	**0.41**	**4.73**	**0.19**
1423	*ccmM*	Carbonate dehydratase	1.07	**0.19**	**0.22**	**6.43**	**1.93**
1424	*ccmN*	CO_2-concentrating mechanism protein	1.07	1.13	0.61	**3.64**	0.67
0284		CO_2-concentrating mechanism protein CcmK	0.71	**0.24**	1.08	1.09	**0.04**
0285		CO_2-concentrating mechanism protein CcmK	0.84	**0.47**	0.80	0.92	**0.34**
1425	*ccmO*	CO_2-concentrating mechanism protein CcmO	1.43	0.56	**1.90**	1.72	**0.36**
Rubisco and carbonic anhydrase							
1426	*rbcL*	Ribulose bisphosphate carboxylase large subunit	1.64	**0.17**	**0.50**	**2.57**	0.81
1535	*rbcX*	Possible Rubisco chaperonin	0.68	1.55	1.00	0.57	1.49
1427	*rbcS*	Ribulose 1,5-bisphosphate carboxylase small subunit	1.69	**0.06**	**0.50**	**3.03**	**0.11**
1447	*icfA*	Carbonate dehydratase	**2.37**	1.44	**0.38**	**2.81**	1.31
Regulatory proteins							
0565		Two-component sensor His kinase (FHA domain)	**4.29**	**8.72**	0.69	1.16	1.64
1557	*rpoD6*	Group 2 RNA polymerase σ factor RpoD6	**3.49**	**0.16**	**2.07**	0.92	**2.54**
0569	*rpoD4*	Group 2 RNA polymerase σ factor RpoD4	**3.37**	1.40	1.67	1.16	0.98
General stress proteins							
0243	*hliC*	Lhc-like protein Lhl4	**5.50**	**0.31**	**17.79**	**3.10**	**0.12**
0297	*ftsH*	ATP-dependent zinc protease	**4.77**	**0.51**	1.78	1.78	**2.00**
1809	*flv3*	Flavoprotein (Flv3 homolog in 6803)	**3.97**	**2.30**	1.26	1.66	**0.43**
1997	*hliA*	Possible high light-inducible protein	**3.97**	**0.12**	**2.67**	1.39	**0.09**
0893	*psbAIII*	PSII q(b) protein	**3.87**	**0.13**	1.74	**5.69**	**0.22**
1389	*psbAII*	PSII q(b) protein	**3.37**	**0.05**	1.82	**4.55**	**0.28**
1822		Putative lipoprotein	**3.52**	1.44	**3.07**	1.06	0.87
Genes with higher transcript levels for proteins of unknown function							
0418		Unknown protein	**5.99**	0.65	**5.41**	1.60	1.47
2529	*gifB*	Hypothetical protein	**5.49**	**0.37**	0.89	1.30	**0.02**
0900	*gifA*	Hypothetical protein	**5.02**	1.17	0.95	**3.16**	**0.49**
1476		Hypothetical protein	**3.85**	**0.20**	0.73	**3.92**	**0.41**
0318		Hypothetical protein	**3.83**	1.63	0.71	1.68	1.22
0014		Hypothetical protein	**3.54**	**6.41**	1.18	**1.90**	**2.80**

mutant cells. Whether instead of 2OG another metabolite specifically induced by LC conditions, such as 2PG (Marcus et al., 1983; Eisenhut et al., 2008a; Kaplan et al., 2008; Nishimura et al., 2008), or another internal signal, such as the internal pool of C_i, as suggested by Woodger et al. (2005), serves as the signal to induce the LC-specific acclimation processes needs additional investigation.

Comparison of LC-Induced Changes in the Transcriptome between Cells of the Wild Type and the PII Mutant

The differences in the metabolome between the wild type and the MP2 mutant can be expected to be, to a large extent, the result of changes in the transcription of genes for specific enzymes of the central C and N metabolism. For example, the mRNA levels of genes for the TCA cycle enzymes citrate synthase (*orf0612*) and fumarate hydratase (*orf1007*), as well as the malic enzyme (*orf1297*) and one subunit of the pyruvate dehydrogenase complex (*orf0143*), are 2- to 3-fold decreased, corresponding to the reduced level of TCA cycle intermediates in HC cells of the mutant MP2 (Table I; Fig. 4). Moreover, one of the N-assimilating Gln synthetases (*orf2156*) showed 4-fold lower transcript amounts in HC-grown cells of the mutant MP2 compared with the wild type. In contrast, genes for a few enzymes in the glycolysis and 2PG metabolism showed higher mRNA levels in mutant cells compared with the wild type (e.g. the *orf2078* for one phosphoglycerate mutase is expressed approximately 9-fold higher). Interestingly, a 15-fold higher mRNA amount was found for *orf2078* in wild-type cells 24 h after the LC shift, whereas in the mutant, it was only increased 2-fold. Obviously, the transcripts for this gene are already increased at HC conditions in MP2, as in the wild type when shifted into LC. Similarly, the mRNA for the T-protein subunit gene (*orf2308*) of the Gly decarboxylase increases in wild-type cells only after a LC shift but is found at higher levels in cells of the mutant MP2 at HC.

Despite the finding that the majority of transcriptional changes of genes for enzymes of the central C and N metabolism are similar in wild-type and mutant cells after the HC-to-LC shift (Table I), the observed differences in gene expression and metabolite concentrations between wild-type and MP2 cells at HC conditions further confirm the inability of the PII-defect mutant to correctly recognize the proper C-N ratio. In particular, genes and metabolites involved in N assimilation are at lower levels compared with the wild type. Possibly, the incorrect sensing of the C-N ratio may explain the suboptimal performance of mutant cells at HC conditions (Fig. 1A).

General Changes in the Transcriptome of *Synechococcus* 7942 during LC Acclimation

Beyond the clear effects on primary metabolism discussed so far, the high impact of the HC-to-LC shift on the metabolism of *Synechococcus* 7942 is well displayed by the system-wide DNA microarray data (for the whole data set, see Supplemental Table S2). While metabolomic phenotyping has been restricted to a subset of the total metabolite spectrum detectable by GC-MS, the transcriptomic changes are representative of the whole genome. Approximately 40 genes showed higher (more than 3-fold) transcript levels, whereas the amount of mRNA for 100 genes is more than 3-fold decreased in wild-type cells 6 h after the shift to LC conditions (Fig. 5A). Most of the genes whose expression increased code for proteins involved in C metabolism, photosynthesis, and electron transport, whereas the genes with decreased expression code for proteins involved in N assimilation and protein synthesis. About the same number of hypothetical and unknown proteins also showed changed expression (Fig. 5A). A remarkably low number of genes for stress proteins are differentially regulated after the HC-to-LC shift in wild-type cells. The number of genes with increased transcript levels and the general functions of the gene products are almost identical in cells of the mutant MP2 when shifted for 6 h to LC conditions, as found in wild-type cells (Fig. 5B). However, only a few genes showed more than 3-fold decreased mRNA levels in MP2 cells. Obviously, many of the genes characterized by lower transcript levels in LC-shifted wild-type cells are already expressed at a lower level in HC-grown MP2 cells (Fig. 5C). Again, the PII sensor system appears to have a limited influence on C-specific gene expression alterations but functions specifically to reduce N assimilation under the chosen experimental conditions.

Genes coding for proteins involved in the active uptake of C_i (bicarbonate and/or CO_2) as part of the CCM showed the highest increase in transcript levels 6 h after the LC shift, as was found previously by reverse transcription-PCR and northern-blot hybridization in *Synechococcus* species (Woodger et al., 2003, 2007) and in *Synechocystis* 6803 (Wang et al., 2004; Eisenhut et al., 2007). The strongest responses are found for the bicarbonate-specific ATP-binding cassette transporter BCT1 and the symporter SbtA (Table II). As reported before (Shibata et al., 2001; Zhang et al., 2004; Battchikova and Aro, 2007), the NDH1 complex is differentially composed of cells grown in HC (constitutive NDH1 complex with nonregulated subunits, e.g. NdhF4 and NdhD4), whereas an additional CO_2-converting NDH1 complex is activated under LC (e.g. NdhD3; Table II), as was reported previously (Woodger et al., 2003). However, these LC-induced transcript levels are clearly not controlled by the PII-based C-N sensor system, since the changes are similar in the wild type and the MP2 mutant (Table II). As found previously in *Synechocystis* 6803 (Eisenhut et al., 2007), genes for the carboxysomal proteins and Rubisco are not significantly increased 6 h after the LC shift, with the exception of carbonic anhydrase. However, *ccmK*, *ccmM*, and *rbcL* showed transient increases in mRNA levels when cells of *Synechococcus* 7942 were analyzed during the first 60 min after a shift to CO_2-free air (Woodger et al., 2003). In long-term (24 h) LC-acclimated cells, most of the genes for C_i transport return to the control level, whereas the genes for the carboxysome showed decreased transcript levels despite the increased CCM activity and the increased number of this prokaryotic organelle in LC cells (McKay et al., 1993; Savage et al., 2010). The decreased expression of carboxysome shell proteins reflects the lowered growth rate of the cells in

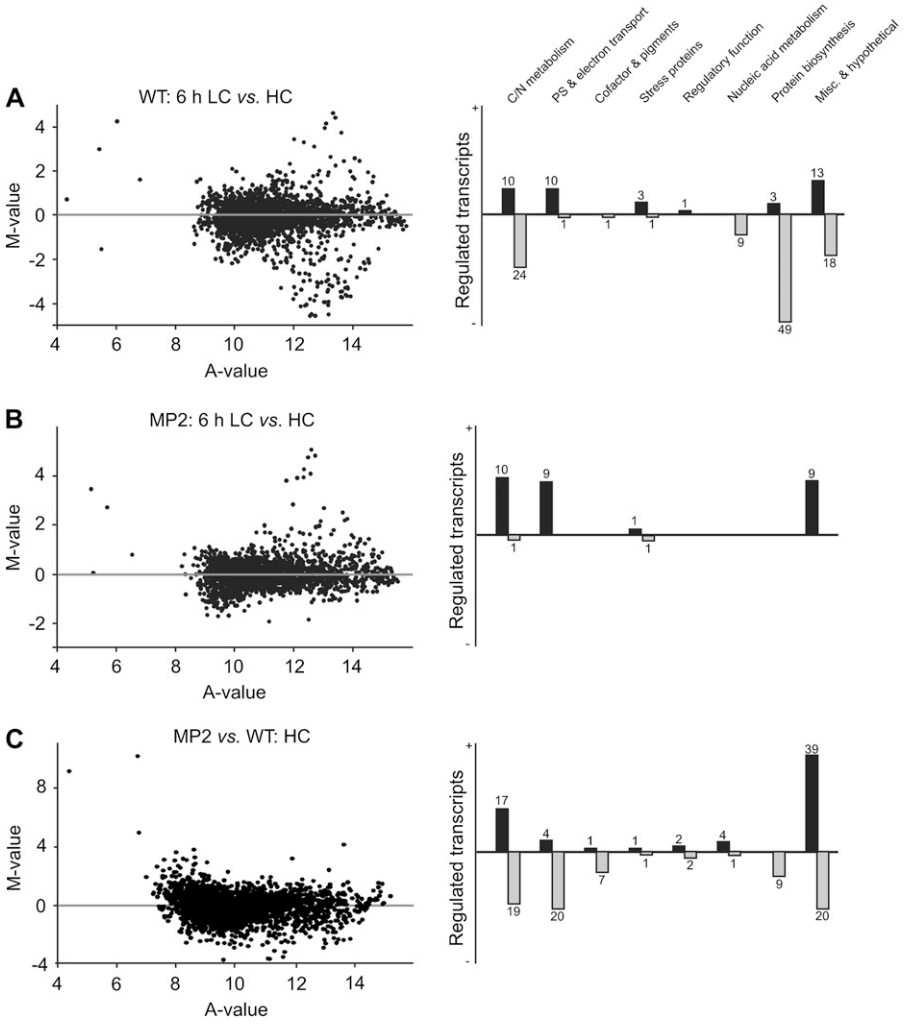

Figure 5. Scatterplots of differentially regulated transcripts (left panels) and distribution of the genes in different metabolic categories (3-fold increase or decrease in transcript levels; right panels). A and B, Data for the *Synechococcus* 7942 wild type (WT; A) or the PII mutant (MP2; B) in response to a shift for 6 h into LC (0.035% CO_2) compared with HC conditions (5% CO_2). C, Comparison of the mutant MP2 and the wild type after long-term acclimation to HC (5% CO_2). A value, Fluorescence intensity of a single gene; M value, relative expression change of a single gene under the mentioned conditions, calculated as $\log_2$ value of the ratio of the A values.

LC conditions, which involves decreasing the rate of new synthesis of the carboxysomal proteins.

In addition to genes for proteins annotated with functions in the CCM (Table II) and defined enzymatic steps in the central C and N metabolism (Table I), many additional genes were differentially regulated in wild-type cells in different C_i conditions (Supplemental Table S2). Among the most highly LC-induced genes, we found many that coded for hypothetical proteins and a few general stress proteins (e.g. *hliA* and *hliC*, *flv3*, *psbAII*, and *psbAIII*; Table II). An increased transcript level of genes for PSII subunits, *psbAII*, *psbAIII*, and *psbDII*, was also shown by Woodger et al. (2003) in LC-shifted cells of *Synechococcus* 7942. Many of these genes are known to be also induced by high light and LC in *Synechocystis* 6803 (Hihara et al., 2001; Wang et al., 2004; Eisenhut et al., 2007) or were found to be induced after iron starvation in *Synechococcus* 7942 (Nodop et al., 2008). Interestingly, we did not find increased transcript levels for genes of PSI in LC-shifted *Synechococcus* 7942 cells. Some of the PSI genes showed slightly decreased mRNA amounts, as shown previously for the *psaE* gene encoding the stroma-exposed protein of PSI (Woodger et al., 2003), whereas the PSI gene transcripts were coordinately increased in LC-treated cells of *Synechocystis* 6803 (Eisenhut et al., 2007). The activation of PSI in LC-treated cells of *Synechocystis* 6803 was interpreted as increased cyclic electron transport activity necessary to energize the CO_2 conversion to bicarbonate at the alternative NDH1 complex (Eisenhut et al., 2007). *Synechococcus* 7942 obviously follows a different strategy to connect the LC-stimulated NDH1 complex to photosynthetic or respiratory electron transport.

In addition to the approximately 40 genes with higher mRNA levels at 6 h after the LC shift (Fig. 5A), there are approximately 100 genes that show a significantly reduced transcript amount (Supplemental Table S2). The genes characterized by decreased mRNA levels mainly belong to three groups. The highest depression (20- to 3-fold) was observed for approximately 40 genes that encode ribosomal proteins and other parts of the translational machinery, which reflects the rapid and continued necessity to save energy and to decrease the growth rate of LC-acclimated cells. A second group of strongly depressed genes encodes proteins involved in coordinating N assimilation to the availability of C. These

effects are clearly visible for genes of the ammonium (*orf0442*) and nitrate transport systems (*nrt* operon, e.g. *orf1239*), nitrite reductase (*orf1240*), and Gln synthetase (*orf2156*). Finally, mRNAs of many genes for proteins of unknown function are also less abundant in LC-treated cells (Supplemental Table S2).

Transcriptomic Changes in Comparison of the Wild Type and the PII Mutant

Generally, more differences between the wild type and the MP2 mutant exist among the genes with decreased transcript levels, whereas the genes with increased transcript levels were almost identical in wild-type and PII mutant cells of *Synechococcus* 7942 after the HC-to-LC shift. Most of the CCM genes behaved identically (Table II). The few but perhaps highly important differences may enhance our understanding of the regulatory role of PII. For example, some of the genes characterized by higher mRNA levels in wild-type cells after the LC shift are found constitutively at higher transcript levels in cells of the PII mutant at HC conditions (e.g. *orf0217* for 2PG phosphatase, *orf2308* for T-protein of the Gly cleavage system, *ofr1939* for one glyceraldehyde-3-phosphate dehydrogenase isoform, *ofr2078* for one 3PGA mutase [Table I] and *ndhF3* [Table II]). Additionally, many of the genes that code for N assimilatory proteins showed lowered transcript amounts in the PII mutant at HC, whereas wild-type cells decrease their expression only after the LC shift (Tables I and III). Apparently, the mutant has become less sensitive or nonresponsive to some of the signals that indicate HC.

As discussed above for the changes in metabolite amounts, part of the HC-to-LC acclimation response of *Synechococcus* 7942 is deregulated in cells of the PII mutant. The transcriptomes of wild-type and PII mutant cells grown at HC conditions are quite different: compared with the wild type, more than 60 genes showed higher transcript levels and approximately 80 genes showed lower transcript levels in cells of the PII mutant under steady-state growth at HC conditions (Fig. 5C). As clearly revealed by the genes showing the most pronounced differences (i.e. more than 5-fold increased or decreased transcript levels), the MP2 mutant at HC seems to partly display a gene-expression status characteristic of the LC-acclimated wild type. It should be noted, however, that the CCM-related genes are similarly regulated in wild-type and MP2 mutant cells. Most of the genes that showed higher transcript levels in HC-grown cells of MP2, compared with the wild type, were previously found to be among the genes showing increased mRNA amounts in LC-shifted wild-type-cells (i.e. genes showing higher expression in the PII mutant at HC become induced in wild-type cells 6 or 24 h after the LC shift, whereas their LC stimulation is missing or much lower in cells of the PII mutant). In agreement with these data, genes with decreased transcript levels in cells of the PII mutant compared with the wild type at HC showed reduced mRNA levels in wild-type cells after LC shifts (Table III). Among the genes with lower transcript levels, we found many examples of subunits of the phycobilisomes, which correlates with the diminished pigmentation of the PII mutant (Fig. 1B) and the known function of reduced phycobilisome production as a N-saving measure in N-starved cyanobacterial cells (Forchhammer and Tandeau de Marsac, 1995; Sauer et al., 2001).

CONCLUSION

Changing amounts of C_i have a great impact on the metabolism of *Synechococcus* 7942 (Fig. 3). Metabolic phenotyping revealed a general change among intermediates of the central C as well as N metabolism, which results mainly from a redirection of organic C fixed by the Calvin-Benson cycle from storage (Suc and glycogen) toward C catabolism via glycolysis, OPP, and the incomplete TCA cycle. In parallel, photorespiratory 2PG metabolism is activated. However, during the first few hours after the shift from HC to LC, we also found clear indications that not only C but also new N assimilation is at least transiently repressed, possibly because it is the second largest energy- and C-demanding cellular process. Comparable changes have been found in leaves of the plant Arabidopsis after shifts to lower CO_2 concentrations, when C storage as well as N assimilation diminished (Arrivault et al., 2009). At the metabolic level, the reduced N assimilation is best distinguished by the relative increase of the TCA cycle intermediates succinate and 2OG, whereas the primary N assimilation products Gln and Asp are diminished.

While the LC shift-induced changes in metabolites of the central C metabolism were also found in cells of the PII mutant, marked differences in the alterations of TCA cycle intermediates and amino acids were detected. Cells of the PII mutant under HC conditions already displayed features of LC-treated wild-type cells, which is not only reflected in reduced growth and pigmentation but also in significantly lowered Gln and Asp levels. The metabolic phenotyping provided further evidence that the PII signaling system is indeed involved in the acclimation to different C_i conditions; however, it appears to be mostly involved in the regulation of processes linked to the energy-consuming N assimilation that was reduced after LC shifts. Our results indicate that the N assimilation is locked into the LC state in cells of the MP2 mutant of *Synechococcus* 7942 even after long-term growth at HC conditions.

Our interpretation of the metabolic changes was well supported by the measured alterations in the relative transcript levels of genes using a DNA microarray for the whole *Synechococcus* 7942 genome (Table I; Fig. 3). The changed expression of genes for enzymes of the central C and N metabolism is part of the general redirection of gene expression during LC acclimation by *Synechococcus* 7942 (Fig. 3). Genes for C_i transporters were found to be highly activated in order to deal with the reduced CO_2 supply, whereas those for the structure

Table III. *Relative transcriptional changes (MP2-HC/WT-HC) of genes in cells of the Synechococcus 7942 PII mutant (MP2) compared with the wild type grown at HC (5% CO_2) conditions*

Only genes are displayed that show a more than 5-fold increase or decrease in transcript levels in cells of the PII mutant compared with the wild type (WT) at HC conditions. For comparison, the relative expression changes of these genes are also shown in cells of the wild type and the PII mutant after 6- and 24-h shift to LC conditions, respectively. Significantly increased or decreased transcript levels are shown in bold.

Gene	Annotation	WT-LC/WT-HC		MP2-HC/ WT-HC	MP2-LC/MP2-HC	
		6 h	24 h		6 h	24 h
Genes showing more than 5-fold increased transcript levels in the PII mutant						
0243	Lhc-like protein Lhl4	**5.50**	**0.31**	**17.79**	**3.10**	**0.12**
2071	Hypothetical protein	0.83	**12.44**	**14.06**	1.10	**2.61**
1572	Dehydrogenase subunit-like protein	0.63	**4.50**	**12.36**	0.70	**2.31**
2356	Transcriptional regulator CRP family protein	1.42	**11.56**	**9.85**	0.88	**2.51**
2127	NblA protein	1.89	0.67	**9.30**	0.79	0.69
2078	Phosphoglycerate mutase	0.58	**15.42**	**8.78**	1.08	**1.90**
1688	Sulfate ATP-binding cassette transporter, permease protein CysW	**2.02**	**14.60**	**8.62**	0.58	**3.02**
0725	Helicase	**2.86**	**27.29**	**8.44**	1.77	**6.80**
2164	Cell death-suppressor protein Lls1 homolog	0.99	**7.85**	**7.72**	0.93	1.49
0617	Hypothetical protein	1.58	**9.11**	**7.37**	0.74	1.21
0479	Hypothetical protein	0.78	**3.72**	**6.61**	1.00	**9.88**
0312	Hypothetical protein	1.34	**11.10**	**6.30**	**0.42**	1.66
0418	Unknown protein	**5.99**	0.65	**5.41**	1.60	1.47
1576	H^+/Cl^- exchange transporter ClcA.	0.62	**3.11**	**5.29**	0.90	**4.21**
Genes showing more than 5-fold decreased transcript levels in the PII mutant						
0328	Phycobilisome anchor protein ApcE	1.04	0.63	**0.07**	**2.31**	**0.40**
1050	Phycocyanin linker protein 33K	1.03	0.56	**0.08**	0.99	1.87
0325	Allophycocyanin linker protein	0.95	**0.09**	**0.09**	**3.49**	**0.08**
1049	30-kD rod-linker	1.22	**0.19**	**0.11**	1.00	**0.07**
1120	Heme oxygenase	**0.50**	**0.09**	**0.12**	0.96	**0.28**
0326	Allophycocyanin, β-subunit	1.62	**0.33**	**0.14**	1.65	**2.52**
2157	Hypothetical protein	**0.25**	**0.34**	**0.14**	0.73	1.38
0335	ATP synthase F1, δ-subunit	**0.23**	**0.24**	**0.15**	1.48	**0.12**
0920	PSI reaction center subunit X	**0.39**	0.95	**0.16**	**2.04**	1.17
0407	PSI reaction center subunit X	0.59	0.61	**0.16**	1.68	0.85
0578	Sulfolipid biosynthesis protein	0.96	**0.50**	**0.16**	1.23	1.03
0535	PsaC	**0.26**	**0.29**	**0.17**	**2.01**	0.90
1131	Ferredoxin thioredoxin reductase variable α-chain	0.47	0.99	**0.17**	0.93	**0.36**
1987	Hypothetical protein	**0.24**	**0.29**	**0.17**	0.92	1.12
1052	Phycocyanin, β-subunit	0.65	**0.07**	**0.17**	1.21	0.21
1492	Hypothetical protein	1.03	1.15	**0.17**	1.24	0.69
0505	Fru-1,6-bisphosphatase, class II (EC 3.1.3.11)	**0.30**	**0.08**	**0.17**	1.11	**0.31**
1250	PSI reaction center subunit III precursor (PSI-F)	0.82	**0.50**	**0.17**	**1.93**	1.62
1891	Hypothetical protein	1.11	0.96	**0.18**	1.31	**0.24**
2343	PSI reaction center subunit VIII-related protein	**0.49**	**0.45**	**0.18**	1.88	**3.53**
1383	Inorganic pyrophosphatase	0.71	**0.27**	**0.18**	1.39	**2.54**
2210	30S ribosomal protein S11	**0.07**	**0.31**	**0.18**	0.75	0.80
0789	Unknown protein	1.04	0.64	**0.19**	0.95	**0.44**
0383	Hypothetical protein	0.99	0.89	**0.19**	1.04	**2.02**
1792	δ-Aminolevulinic acid dehydratase (EC 4.2.1.24)	**0.33**	0.75	**0.20**	0.87	**2.83**
0694	30S ribosomal protein S1	**0.12**	**0.01**	**0.20**	0.93	0.03
1736	FeS assembly ATPase SufC	**0.48**	0.57	**0.20**	0.95	0.60
1053	Phycocyanin, α-subunit	0.83	**0.02**	**0.20**	1.10	**0.17**
0327	AP α-apoprotein (AA 1-161)	1.58	**0.13**	**0.20**	**2.39**	**2.91**

of the carboxysome hardly changed. Again, the main difference between PII mutant and wild-type cells was found in the LC shift-induced expression changes for genes involved in N assimilation or use. The reduced mRNA levels of genes for N assimilation and the N-storing phycobilisome proteins were already detectable in cells of the PII mutant under HC conditions. Moreover, many other genes are differentially regulated between PII mutant and wild-type cells under HC conditions. Interestingly, the transcript levels of most of them increased in wild-type cells after the LC shift. The characterization of the transcriptome also revealed a global influence of the PII protein on these changes, but the specifically C_i-related changes in gene expression (i.e. differentially regulated genes for CCM components) are much less affected than those for N assimilation-

related proteins or for unknown processes. These results support the view that the PII protein is an important cellular sensor of the N-C ratio. However, it seems to be primarily regulating the expression of genes for proteins specifically involved in the regulation of N assimilation, such as NtcA (Forchhammer, 2008; Llácer et al., 2010). Interestingly, the decreased N assimilation in *Synechococcus* 7942, which is similar to that reported for *Synechocystis* 6803 (Wang et al., 2004; Eisenhut et al., 2007), was found in cells accumulating 2OG, pointing to another metabolic sensor specific for changes in the C metabolism in LC-treated cells. Such a sensory mechanism may not only play a role in low-CO_2 acclimation among cyanobacteria but also in higher plants, which harbor a PII signaling system of comparable structure and function (e.g. in the regulation of Arg biosynthesis; Feria Bourrellier et al., 2009) in chloroplasts.

MATERIALS AND METHODS

Cyanobacterial Strains and Growth Conditions

Synechococcus sp. strain PCC 7942 was obtained from the Institute Pasteur, Collection Nationale de Cultures de Microorganismes, and served as the wild type. The *Synechococcus* 7942 mutant with a defective PII protein, MP2 or Δ*glnB*::Km, was constructed by Forchhammer and Tandeau de Marsac (1995). For all experiments, axenic cultures of the cyanobacteria were grown photoautotrophically in batch cultures at an optical density at 750 nm (OD_{750}) of approximately 1.0 (equivalent to approximately 10^9 cells mL^{-1}), as described in detail by Eisenhut et al. (2008a). Cells were routinely cultivated by aeration with CO_2-enriched air (5% CO_2, defined as HC) at 29°C under continuous illumination of 100 μmol photons m^{-2} s^{-1} (warm white light; Osram L58 W32/3) in BG11 medium (Rippka et al., 1979) buffered with TES-(TES)-KOH (20 mM final concentration) at pH 8.0. C_i limitation was set by transferring the conditions of exponentially growing cells to bubbling with ambient air (approximately 0.035% CO_2, defined as LC) in BG11 medium buffered with TES-KOH at pH 7.0. Growth was monitored by measuring the OD_{750}. Cultivation of the mutant was performed at 20 μg mL^{-1} kanamycin. Contamination by heterotrophic bacteria was checked by spreading 0.2 mL of culture on Luria-Bertani plates. All experiments were repeated using at least three independent cultivations.

Physiological Characterization

To characterize growth, cell suspensions of *Synechococcus* 7942 wild type and the MP2 mutant were harvested by centrifugation (4,000*g* at 20°C) and adjusted to an OD_{750} of 0.6 with fresh medium. Subsequently, the strains were cultivated for 9 d with daily dilution to the initial OD_{750} of 0.6. Growth and pigmentation were followed by absorption measurements every 24 h. The content of the photosynthetic pigments chlorophyll *a*, phycocyanin, and carotenoids was calculated from the absorption measurements as described by Sigalat and de Kouchkowski (1975). The rate of CO_2-dependent oxygen evolution as a function of C_i concentration was determined using a Clark-type oxygen electrode (Hansatech) as described by Eisenhut et al. (2008b). The photosynthetic rates were measured by adding defined amounts of C_i to concentrated cell suspensions (chlorophyll *a* content of approximately 10 μg mL^{-1}, equal to an OD_{750} of approximately 2.3) at a light intensity of 300 μmol photons m^{-2} s^{-1}.

Metabolomic Phenotyping

Sampling of cells was done as described in detail by Eisenhut et al. (2008a). Briefly, 5 to 10 mL of cells was separated from the medium by filtration (0.45-μm nitrocellulose filters; Schleicher & Schuell) in the light without any subsequent washing. The cell pellets on the filters were immediately frozen in liquid N and stored at −80°C. Time until metabolic inactivation by freezing was approximately 20 s. Subsequently, metabolites were extracted from deep-frozen cells by 80% methanol containing a defined amount of the internal standards nonadeconoic acid methylester (0.17 mg mL^{-1}) and ribitol (0.017 mg mL^{-1}). In succession, chloroform and water were added to separate polar and lipophilic metabolites by phase separation. The phase containing the polar metabolites was dried by vacuum centrifugation. The extracted compounds were derivatized by methoxyamination and subsequent trimethylsilylation (Fiehn et al., 2000). The mixtures were separated on a 6890-N gas chromatograph (Agilent), and mass spectrometric data were acquired through a Pegasus III time of flight mass spectrometer as described by Eisenhut et al. (2008a). The GC-time of flight-MS chromatograms were processed by TagFinder software (Luedemann et al., 2008). Compounds were identified by comparison with a reference library of mass spectra and retention indices from the collection of the Golm Metabolome database (Hummel et al., 2010). The resulting data set of the identified metabolites may be found in Supplemental Table S1. The analysis was done with three biological replicates with two technical replicates of each sample.

Transcriptomic Phenotyping

Sampling of cells was done as described in detail by Eisenhut et al. (2007). Briefly, cells from a 10-mL suspension were harvested by centrifugation at 4,000*g* for 3 min at 4°C and were immediately frozen at –80°C. Total RNA was extracted by the High Pure RNA Isolation Kit (Roche Diagnostics). The same RNA samples were used for labeling in DNA microarray experiments and for reverse transcription-PCR. cDNA synthesis and labeling, microarray hybridization, and microarray data evaluation were done as described by Nodop et al. (2008). Briefly, 10 μg of total RNA was used for cDNA synthesis. Cy3- and Cy5-*N*-hydroxysuccinimidyl ester dyes were introduced during the first-strand cDNA generation. Equal amounts of labeled cDNA were mixed and hybridized to a whole-genome *Synechococcus* 7942 microarray. The array is composed of 2,989 genes. For each gene, specific 70-mer oligonucleotide probes were printed in four replicates (Nodop et al., 2008). Hybridization was performed in EasyHyb hybridization solutions (Roche) for 90 min at 45°C. After washing, the arrays were scanned by the LS Reloaded microarray scanner (Tecan Trading). Mean signal and mean background intensities were obtained for each spot using the ImaGene Software 6.0 (BioDiscovery). Normalization and *t* statistics were determined using the EMMA 2.2 microarray data-analysis software (Dondrup et al., 2003). The fold change value was calculated as described by Nodop et al. (2008). The resulting data set of the gene expression levels is shown in Supplemental Table S2. Each experiment was performed with RNA from three biological replicates, two technical replicates, and one dye swap.

Supplemental Data

The following materials are available in the online version of this article.

Supplemental Table S1. Complete list of the identified metabolites by GC-MS.

Supplemental Table S2. Relative changes (fold change and SD) of transcript levels in cells of the *Synechococcus* species.

ACKNOWLEDGMENTS

The technical assistance of Klaudia Michl is greatly appreciated.

Received November 30, 2010; accepted January 28, 2011; published January 31, 2011.

LITERATURE CITED

Arrivault S, Guenther M, Ivakov A, Feil R, Vosloh D, van Dongen JT, Sulpice R, Stitt M (2009) Use of reverse-phase liquid chromatography, linked to tandem mass spectrometry, to profile the Calvin cycle and other metabolic intermediates in Arabidopsis rosettes at different carbon dioxide concentrations. Plant J **59:** 826–839

Badger MR, Price GD, Long BM, Woodger FJ (2006) The environmental plasticity and ecological genomics of the cyanobacterial CO_2 concentrating mechanism. J Exp Bot **57:** 249–265

Battchikova N, Aro EM (2007) Cyanobacterial NDH-1 complexes: multiplicity in function and subunit composition. Physiol Plant **131:** 22–32

Campbell L, Liu HB, Nolla HA, Vaulot D (1997) Annual variability of phytoplankton and bacteria in the subtropical North Pacific Ocean at Station ALOHA during the 1991–1994 ENSO event. Deep-Sea Res **44:** 167–192

Cooley JW, Howitt CA, Vermaas WF (2000) Succinate:quinol oxidoreductases in the cyanobacterium *Synechocystis* sp. strain PCC 6803: presence and function in metabolism and electron transport. J Bacteriol **182:** 714–722

Cot SS, So AK, Espie GS (2008) A multiprotein bicarbonate dehydration complex essential to carboxysome function in cyanobacteria. J Bacteriol **190:** 936–945

Dondrup M, Goesmann A, Bartels D, Kalinowski J, Krause L, Linke B, Rupp O, Sczyrba A, Pühler A, Meyer F (2003) EMMA: a platform for consistent storage and efficient analysis of microarray data. J Biotechnol **106:** 135–146

Eisenhut M, Huege J, Schwarz D, Bauwe H, Kopka J, Hagemann M (2008a) Metabolome phenotyping of inorganic carbon limitation in cells of the wild type and photorespiratory mutants of the cyanobacterium *Synechocystis* sp. strain PCC 6803. Plant Physiol **148:** 2109–2120

Eisenhut M, Ruth W, Haimovich M, Bauwe H, Kaplan A, Hagemann M (2008b) The photorespiratory glycolate metabolism is essential for cyanobacteria and might have been conveyed endosymbiotically to plants. Proc Natl Acad Sci USA **105:** 17199–17204

Eisenhut M, von Wobeser EA, Jonas L, Schubert H, Ibelings BW, Bauwe H, Matthijs HCP, Hagemann M (2007) Long-term response toward inorganic carbon limitation in wild type and glycolate turnover mutants of the cyanobacterium *Synechocystis* sp. strain PCC 6803. Plant Physiol **144:** 1946–1959

Feria Bourrellier AB, Ferrario-Méry S, Vidal J, Hodges M (2009) Metabolite regulation of the interaction between *Arabidopsis thaliana* PII and *N*-acetyl-L-glutamate kinase. Biochem Biophys Res Commun **387:** 700–704

Fiehn O, Kopka J, Dörmann P, Altmann T, Trethewey RN, Willmitzer L (2000) Metabolite profiling for plant functional genomics. Nat Biotechnol **18:** 1157–1161

Flores E, Frías JE, Rubio LM, Herrero A (2005) Photosynthetic nitrate assimilation in cyanobacteria. Photosynth Res **83:** 117–133

Forchhammer K (2004) Global carbon/nitrogen control by PII signal transduction in cyanobacteria: from signals to targets. FEMS Microbiol Rev **28:** 319–333

Forchhammer K (2008) P(II) signal transducers: novel functional and structural insights. Trends Microbiol **16:** 65–72

Forchhammer K, Tandeau de Marsac N (1995) Functional analysis of the phosphoprotein PII (*glnB* gene product) in the cyanobacterium *Synechococcus* sp. strain PCC 7942. J Bacteriol **177:** 2033–2040

García-Domínguez M, Reyes JC, Florencio FJ (1999) Glutamine synthetase inactivation by protein-protein interaction. Proc Natl Acad Sci USA **96:** 7161–7166

Hihara Y, Kamei A, Kanehisa M, Kaplan A, Ikeuchi M (2001) DNA microarray analysis of cyanobacterial gene expression during acclimation to high light. Plant Cell **13:** 793–806

Huege J, Goetze J, Scharz D, Bauwe H, Hagemann M, Kopka J (2011) Modulation of the major paths of carbon in photorespiratory mutants of *Synechocystis*. PLoS ONE **6:** e16278

Hummel J, Strehmel N, Selbig J, Walther D, Kopka J (2010) Decision tree supported substructure prediction of metabolites from GC-MS profiles. Metabolomics **6:** 322–333

Husic DW, Husic HD, Tolbert NE (1987) The oxidative photosynthetic carbon cycle or C2 cycle. CRC Crit Rev Plant Sci **5:** 45–100

Kaneko T, Sato S, Kotani H, Tanaka A, Asamizu E, Nakamura Y, Miyajima N, Hirosawa M, Sugiura M, Sasamoto S, et al (1996) Sequence analysis of the genome of the unicellular cyanobacterium *Synechocystis* sp. strain PCC6803. II. Sequence determination of the entire genome and assignment of potential protein-coding regions. DNA Res **3:** 109–136

Kaplan A, Hagemann M, Bauwe H, Kahlon S, Ogawa T (2008). Carbon acquisition by cyanobacteria: mechanisms, comparative genomics and evolution. *In* A Herrero, E Flores, eds, The Cyanobacteria: Molecular Biology, Genomics and Evolution. Caister Academic Press, Norwich, UK, pp 305–323.

Kaplan A, Reinhold L (1999) CO_2 concentrating mechanisms in photosynthetic microorganisms. Annu Rev Plant Physiol Plant Mol Biol **50:** 539–570

Kelly GJ, Latzko E (1977) Chloroplast phosphofructokinase. II. Partial purification, kinetic and regulatory properties. Plant Physiol **60:** 295–299

Kern R, Bauwe H, Hagemann M (2011) Evolution of enzymes involved in the photorespiratory 2-phosphoglycolate cycle from cyanobacteria via algae toward plants. Photosynth Res (in press)

Knoll AH (2008) Cyanobacteria and earth history. *In* A Herrero, E Flores, eds, The Cyanobacteria: Molecular Biology, Genomics and Evolution. Caister Academic Press, Norwich, UK, pp 1–19.

Knoop H, Zilliges Y, Lockau W, Steuer R (2010) The metabolic network of *Synechocystis* sp. PCC 6803: systemic properties of autotrophic growth. Plant Physiol **154:** 410–422

Lieman-Hurwitz J, Haimovich M, Shalev-Malul G, Ishii A, Hihara Y, Gaathon A, Lebendiker M, Kaplan A (2009) A cyanobacterial AbrB-like protein affects the apparent photosynthetic affinity for CO_2 by modulating low-CO_2-induced gene expression. Environ Microbiol **11:** 927–936

Llácer JL, Espinosa J, Castells MA, Contreras A, Forchhammer K, Rubio V (2010) Structural basis for the regulation of NtcA-dependent transcription by proteins PipX and PII. Proc Natl Acad Sci USA **107:** 15397–15402

Luedemann A, Strassburg K, Erban A, Kopka J (2008) TagFinder for the quantitative analysis of gas chromatography-mass spectrometry (GC-MS)-based metabolite profiling experiments. Bioinformatics **24:** 732–737

Luque I, Forchhammer K (2008) Nitrogen assimilation and C/N balance sensing. *In* A Herrero, E Flores, eds, The Cyanobacteria: Molecular Biology, Genomics and Evolution. Caister Academic Press, Norwich, UK, pp 335–362.

Marcus Y, Harel E, Kaplan A (1983) Adaptation of the cyanobacterium *Anabaena variabilis* to low CO_2 concentration in the environment. Plant Physiol **71:** 208–210

Mayo WP, Elrifi IR, Turpin DH (1989) The relationship between ribulose bisphosphate concentration, dissolved inorganic carbon (DIC) transport and DIC-limited photosynthesis in the cyanobacterium *Synechococcus leopoliensis* grown at different concentrations of inorganic carbon. Plant Physiol **90:** 720–727

McKay RML, Gibbs SP, Espie GC (1993) Effect of dissolved inorganic carbon on the expression of carboxysomes, localization of Rubisco and the mode of inorganic carbon transport in cells of the cyanobacterium *Synechococcus* UTEX 625. Arch Microbiol **159:** 21–29

Muro-Pastor MI, Reyes JC, Florencio FJ (2001) Cyanobacteria perceive nitrogen status by sensing intracellular 2-oxoglutarate levels. J Biol Chem **276:** 38320–38328

Muro-Pastor MI, Reyes JC, Florencio FJ (2005) Ammonium assimilation in cyanobacteria. Photosynth Res **83:** 135–150

Nishimura T, Takahashi Y, Yamaguchi O, Suzuki H, Maeda S, Omata T (2008) Mechanism of low CO_2-induced activation of the *cmp* bicarbonate transporter operon by a LysR family protein in the cyanobacterium *Synechococcus elongatus* strain PCC 7942. Mol Microbiol **68:** 98–109

Nodop A, Pietsch D, Höcker R, Becker A, Pistorius EK, Forchhammer K, Michel KP (2008) Transcript profiling reveals new insights into the acclimation of the mesophilic fresh-water cyanobacterium *Synechococcus elongatus* PCC 7942 to iron starvation. Plant Physiol **147:** 747–763

Norman EG, Colman B (1991) Purification and characterization of the phosphoglycolate phosphatase from the cyanobacterium *Coccochloris peniocystis*. Plant Physiol **95:** 693–698

Omata T, Gohta S, Takahashi Y, Harano Y, Maeda S (2001) Involvement of a CbbR homolog in low CO_2-induced activation of the bicarbonate transporter operon in cyanobacteria. J Bacteriol **183:** 1891–1898

Osanai T, Tanaka K (2007) Keeping in touch with PII: PII-interacting proteins in unicellular cyanobacteria. Plant Cell Physiol **48:** 908–914

Rippka R, Deruelles J, Waterbury JB, Herdman M, Stanier RY (1979) Generic assignments, strain histories and properties of pure cultures of cyanobacteria. J Gen Microbiol **111:** 1–16

Sauer J, Schreiber U, Schmid R, Völker U, Forchhammer K (2001) Nitrogen starvation-induced chlorosis in *Synechococcus* PCC 7942: low-level photosynthesis as a mechanism of long-term survival. Plant Physiol **126:** 233–243

Savage DF, Afonso B, Chen AH, Silver PA (2010) Spatially ordered dynamics of the bacterial carbon fixation machinery. Science **327:** 1258–1261

Shibata M, Ohkawa H, Kaneko T, Fukuzawa H, Tabata S, Kaplan A, Ogawa T (2001) Distinct constitutive and low-CO_2-induced CO_2 uptake systems in cyanobacteria: genes involved and their phylogenetic relationship with homologous genes in other organisms. Proc Natl Acad Sci USA **98:** 11789–11794

Sigalat C, de Kouchkowski Y (1975) Fractionnement et caracterisation de l'algue bleue unicellulaire *Anacystis nidulans*. Physiol Veg **13:** 243–258

Sugita C, Ogata K, Shikata M, Jikuya H, Takano J, Furumichi M, Kanehisa M, Omata T, Sugiura M, Sugita M (2007) Complete nucleotide sequence of the freshwater unicellular cyanobacterium *Synechococcus elongatus* PCC 6301 chromosome: gene content and organization. Photosynth Res **93:** 55–67

Völker U, Hecker M (2005) From genomics via proteomics to cellular physiology of the Gram-positive model organism *Bacillus subtilis*. Cell Microbiol **7:** 1077–1085

Wang HL, Postier BL, Burnap RL (2004) Alterations in global patterns of gene expression in *Synechocystis* sp. PCC 6803 in response to inorganic carbon limitation and the inactivation of *ndhR*, a LysR family regulator. J Biol Chem **279:** 5739–5751

Woodger FJ, Badger MR, Price GD (2003) Inorganic carbon limitation induces transcripts encoding components of the CO_2-concentrating mechanism in *Synechococcus* sp. PCC7942 through a redox-independent pathway. Plant Physiol **133:** 2069–2080

Woodger FJ, Badger MR, Price GD (2005) Sensing of inorganic carbon limitation in *Synechococcus* PCC7942 is correlated with the size of the internal inorganic carbon pool and involves oxygen. Plant Physiol **139:** 1959–1969

Woodger FJ, Bryant DA, Price GD (2007) Transcriptional regulation of the CO_2-concentrating mechanism in a euryhaline, coastal marine cyanobacterium, *Synechococcus* sp. strain PCC 7002: role of NdhR/CcmR. J Bacteriol **189:** 3335–3347

Zhang P, Battchikova N, Jansen T, Appel J, Ogawa T, Aro EM (2004) Expression and functional roles of the two distinct NDH-1 complexes and the carbon acquisition complex NdhD3/NdhF3/CupA/Sll1735 in *Synechocystis* sp PCC 6803. Plant Cell **16:** 3326–3340